

Article

# Influence of Carbon Diffusion and the Presence of Oxygen on the Microstructure of Molybdenum Powders Densified by SPS

Mathias Moser <sup>1,2</sup>, Sylvain Lorand <sup>1</sup>, Florian Bussiere <sup>1</sup>, Frédéric Demoisson <sup>1</sup>, Hervé Couque <sup>2</sup> and Frédéric Bernard <sup>1,\*</sup>

<sup>1</sup> Laboratoire Interdisciplinaire Carnot de Bourgogne, UMR6303 CNRS-Université de Bourgogne-Franche-Comté, BP 47870, 21078 Dijon, France; Mathias\_Moser@etu.u-bourgogne.fr (M.M.); sylvain.lorand@live.fr (S.L.); florian.bussiere@u-bourgogne.fr (F.B.); Frederic.Demoisson@u-bourgogne.fr (F.D.)

<sup>2</sup> Nexter Munitions, 18 route de Guerry, 18000 Bourges, France; h.couque@nexter-group.fr

\* Correspondence: fbernard@u-bourgogne.fr; Tel.: +33-380-396-125

Received: 5 June 2020; Accepted: 8 July 2020; Published: 14 July 2020



**Abstract:** Due to molybdenum's Body-Centered Cubic (BCC) crystalline structure, its ductile–brittle transition temperature is sensitive to shaping, purity and microstructure. Dense molybdenum parts are usually shaped by the powder metallurgy process. The aim of this work concerns the spark plasma sintering of high-purity powders prepared by inductively coupled plasma. The influence of carbon diffusion and its interaction with oxygen on the density (i.e., the densification stage) and on the microstructure (i.e., the grain growth stage) during spark plasma sintering was investigated. The formation of carbide is usually expected for a sintering temperature above 1500 °C leading to grain growth (e.g., more than 10 times larger than the initial powder grain size after sintering at 1900 °C for 10 min). The brittleness was also affected by the segregation of molybdenum carbides at the grain boundaries (i.e., intergranular brittle fracture). Consequently, to reduce the sintering temperature to below 1500 °C, mechanically activated powders were used. From these milled powders, a dense molybdenum disc (60 mm in diameter and 10 mm in thickness) sintered at 1450 °C under a pressure of 70 MPa for 30 min was obtained. It is composed of a fine microstructure without carbide and oxide, its ductility is close to 13% with a maximum resistance of 550 MPa.

**Keywords:** molybdenum; grain growth; carbon diffusion; ball milling; spark plasma sintering

## 1. Introduction

Molybdenum is a refractory metal with a high-temperature resistance, due to its melting point of 2620 °C. Such a characteristic, along with its good mechanical properties, has motivated its use in defense [1] as well as civilian applications, such as the production of ribbons and wires for the lighting industry, electrodes for glass melting and thermal zones for high-temperature ovens. However, its high melting temperature makes the implementation of the material by traditional metallurgy (casting or forging) a complex and expensive process. That is why much research has been conducted into the powder metallurgy of molybdenum [2–4]. However, the sintering process remains complex and long. Indeed, conventional sintering of molybdenum requires temperatures between 1800 and 2000 °C for several hours. In addition, the density obtained from such a sintering process is less than 95% of the theoretical maximum density (TMD) [5,6], which is often not sufficient for target applications such as in defense. Many studies have been performed to increase the density of the end-product by using: (i) different sizes of molybdenum powder [7], (ii) heat treatment of the initial molybdenum powders before sintering [6], (iii) specific additives as densification aids [8], or (iv) alternative methods

of sintering such as explosive consolidation [9,10], microwave energy [11] or spark plasma sintering (SPS) [3,4,7,12,13].

It is well known that the presence of some impurities in molybdenum powder can modify the mechanical behavior of the sintered product. The presence of oxygen influences the mechanical properties by segregating at the grain boundaries [14–16], while other impurities, such as carbon in a reasonable proportion, increase the ductility [17,18], but have a negative effect in excess. Some studies have also investigated the relationship between impurities and the final density. For example, the addition of nickel [19,20] or silicon [21] increases the sinterability of molybdenum leading to a better density of the final product.

Apart from the direct effect of such impurities on the ductility or the density, there is a grain growth phenomenon during the sintering of molybdenum powder at high temperature with a non-negligible effect on the density of the sintered product and, consequently, on the mechanical, electrical and thermal properties. In fact, Lee et al. [22] reported that the concentration of oxygen leading to molybdenum oxide formation is an accelerator factor for grain growth during sintering.

The main objective of this study was to investigate the fabrication by SPS of dense parts starting from powders prepared using inductively coupled plasma technology (ICP). Clearly, it is essential to understand the grain growth and densification stages of such powders in order to control them. Consequently, the present work evaluated several powders and sintering conditions to observe and understand the grain growth and the effects of the presence of oxygen and carbon.

## 2. Experimental Procedure

A 99.95% pure molybdenum powder with a narrow particle size distribution (i.e., D10: 11.04  $\mu\text{m}$ , D50: 16.33  $\mu\text{m}$  and D90: 28.88  $\mu\text{m}$ ) made by the Tekna Company (Macon, France) (i.e., hereafter named Mo-45) was used. This powder was prepared using ICP, which has the advantage of having a high level of sphericity (Figure 1) and a high density ( $10.2 \text{ g} \cdot \text{cm}^{-3}$  obtained by He pycnometry) without any oxide either on the surface of or inside the particle. Scanning Electron Microscope (SEM) images highlight the spherical morphology with regularity in size and shape (Figure 1a). The presence of agglomerated clusters is certainly due to some precursor powder particles not having entirely undergone the spheroidization step because they were expelled too early from the plasma by reflux movements. However, the majority of the grains have smooth surfaces. Despite these few irregularities, two populations of particles were mainly formed: particles with smooth surfaces (Figure 1b) and particles having large facets (Figure 1c). A higher magnification observation shows that the majority of smooth particles are actually composed of large faceted grains covered with a very thin layer on the surface. The smoothing of these particles may be due to faster migration of the surface species during spheroidization than occurred on particles with well-marked facets.

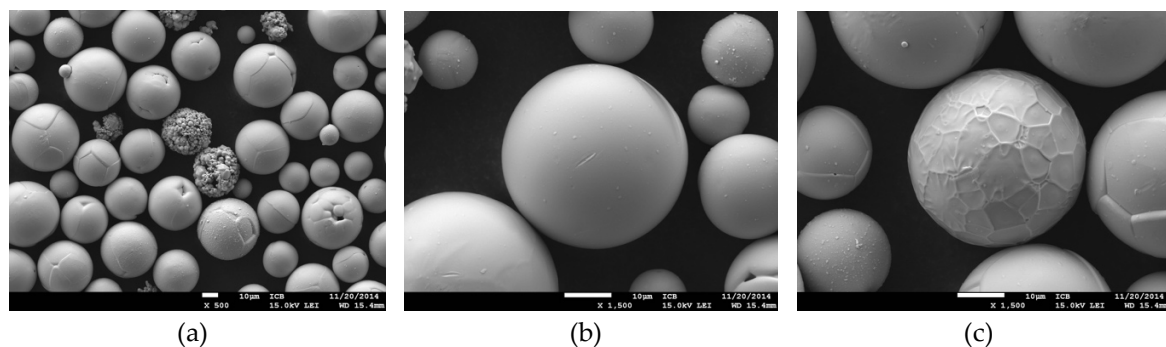


**Figure 1.** (a) SEM image of molybdenum powder Mo-45 (Tekna); (b) and (c) SEM images with a higher magnification showing different powder morphologies.

However, in addition, it is essential to verify the presence on the surface of a native molybdenum oxide. Indeed, some molybdenum oxides,  $\text{MoO}_3$  or  $\text{MoO}_2$ , are usually observed on the very surface of

the powder, due to humidity, but this thin layer can be removed by a thermal treatment at 800 °C under vacuum as proved by XPS (X-ray photoelectron spectroscopy) analysis (Figure 2) performed on Mo-45 powder. XPS spectra are presented of molybdenum powder before (green) and after (red) thermal treatment under vacuum at 800 °C. This study shows that it is not necessary to work under a reducing atmosphere since heating under vacuum at 800 °C is sufficient to remove the thin layer of oxide present on the surface of the molybdenum particles. Indeed, the  $\text{Mo}_{\text{ox}}$   $3d^{3/2}$  peak at 235 eV and the  $\text{Mo}_{\text{ox}}$   $3d^{5/2}$  peak at 232 eV associated with the presence of oxidized molybdenum disappeared in favor of metallic molybdenum after a heat treatment at 800 °C under vacuum (Figure 2). Consequently, as the SPS sintering was also carried out under vacuum, these oxides will be reduced during the heating stage, the rate of which was limited to 50 °C/min for all SPS tests.

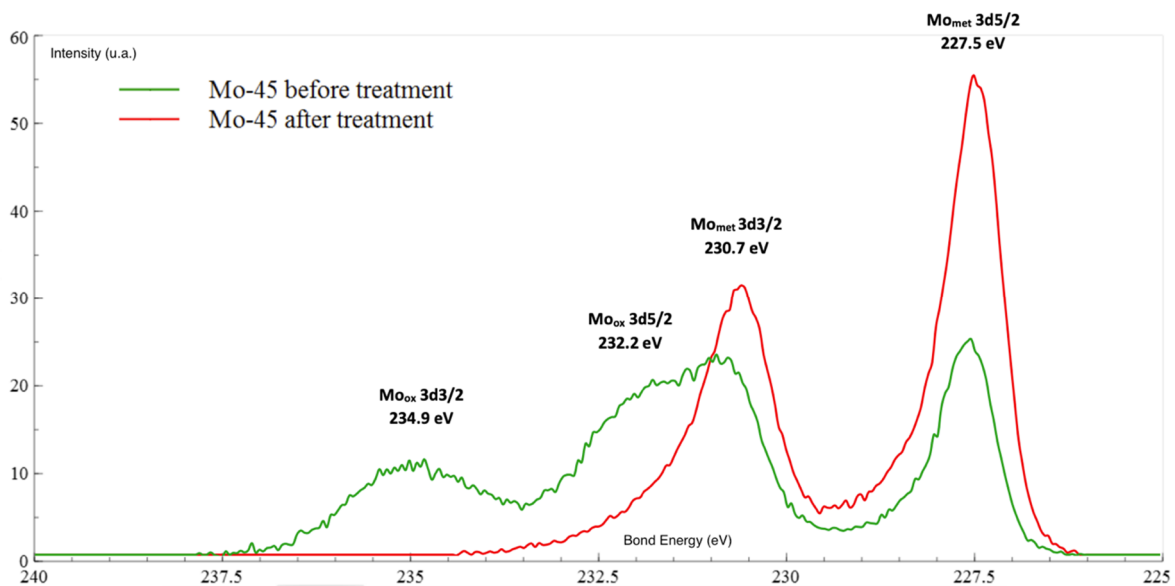


**Figure 2.** XPS spectra of molybdenum powder before (green) and after (red) thermal treatment performed under vacuum at 800 °C.

The SPS assembly used in this work is described in Figure 3a. As molybdenum is a conductive material, the current goes through the sample and, consequently, this latter is heated by Joule effect. To favor this “internal heating”, a spray of boron nitride (BN, an electrical insulating) has been deposited all around the sample (Figure 3c).

A graphite die of 60 mm inner diameter lined with a 0.35 mm thick layer of graphite foil (named Papyex<sup>®</sup>) (Mersen, Gennevilliers, France) was filled with the powder and coated with a boron nitride (BN) spray to prevent radial carbon diffusion (compare Figure 3c with the classical configuration shown in Figure 3b). An additional limit to axial carbon diffusion was provided by 3 mm thick tantalum discs placed between the punches and the powder (Figure 3d). A 3 cm thick layer of graphite felt was wrapped around the die to prevent and limit thermal gradients inside the sample during heating by reducing heat losses by radiation. Sintered samples of 60 mm in diameter and 10 mm in height were then sintered in an FCT HPD-125 spark plasma sintering machine (FCT Systeme, Rauenstein, Germany).

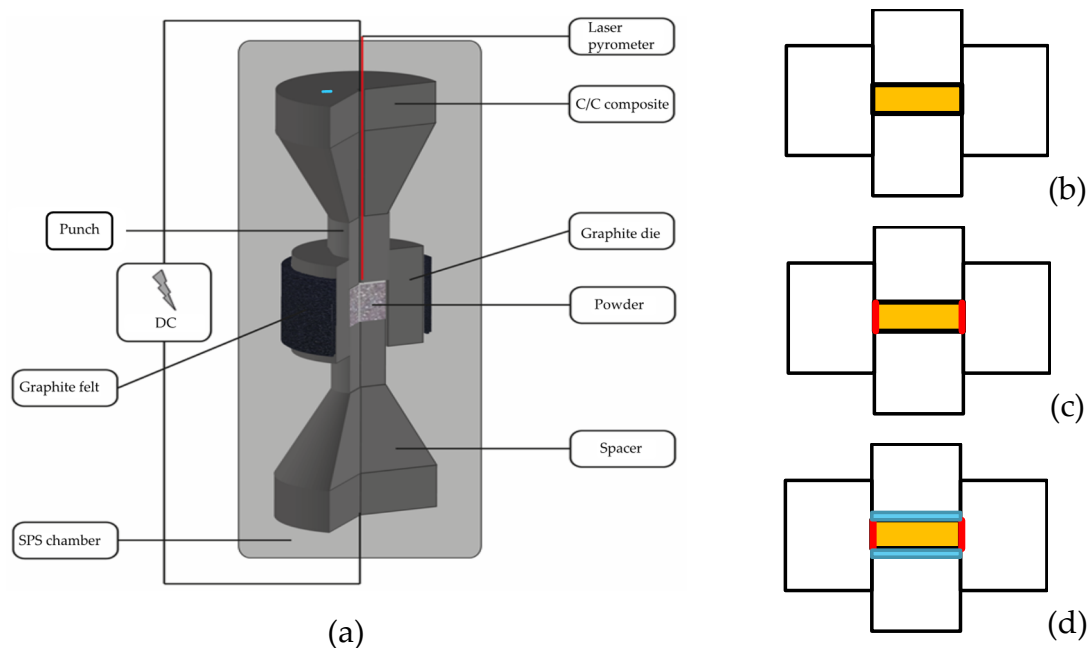


**Figure 3.** (a) General view of spark plasma sintering (SPS) assembly; (b), (c) and (d) represent different sample configurations: (b) classical assembly using graphite foil all around the sample, (c) assembly using a boron nitride (BN) spray on graphite foil around the sample to limit carbon radial diffusion, and (d) assembly with a BN barrier as previously and a tantalum disc (3 mm) on the top and bottom of the powder to limit axial carbon diffusion.

Sintering was carried out under vacuum using a DC electric current ( $\sim 4000$  A) and a heating rate of  $50\text{ }^{\circ}\text{C} \cdot \text{min}^{-1}$ . Above  $400\text{ }^{\circ}\text{C}$ , the temperature was measured and regulated using an optical pyrometer looking at a spot located at 7 mm on the sample top. The temperature was varied from 1750 to  $2000\text{ }^{\circ}\text{C}$  with a hold time at the maximum temperature of between 0 to 30 min. The uniaxial pressure was varied from 28 MPa (the minimum value to ensure sufficient electrical contact) to 90 MPa (the maximum value for graphite tools). The pressure was applied from RT to  $450\text{ }^{\circ}\text{C}$ , just before the activation of the laser pyrometer. To reduce thermal stresses inside the sintered part, it was cooled in a controlled manner at a rate of  $50\text{ }^{\circ}\text{C}/\text{min}$ . Simultaneously, during the cooling, the pressure was slowly decreased at a rate of 6 KN/min. In experiment 10 (see Table 1), two massive discs of tantalum (3 mm thick) located top and bottom of the powder and a BN barrier around the powder (Figure 3d) were used to avoid any carbon diffusion from the graphite into the molybdenum. The sintering conditions for each sample are listed in Table 1.

**Table 1.** Table of sintering conditions of Mo-45 powder.

Experiment No.	Pressure (MPa)	Temperature ( $^{\circ}\text{C}$ )	Holding Time (min)	Protection
1	90	1750	0	BN
2	90	1900	0	BN
3	90	2000	0	BN
4	70	1900	0	BN
5	70	1900	10	BN
6	70	1900	30	BN
7	70	1750	10	BN
8	28	1900	0	BN
9	70 (delayed at $900\text{ }^{\circ}\text{C}$ )	1900	0	BN
10	70	1900	30	BN + Ta

After sintering, the graphite foil on the sample surface was removed by a sanding operation. Two types of preparation for analysis were performed on the sintered parts. First, a transverse cut was made, usually using a circular saw. The relative densities of the sintered molybdenum samples were measured using Archimedes' technique and found to have a value of 10.2. Then, the surface of this slice was mechanically polished, starting with SiC papers down to 3  $\mu\text{m}$  diamond abrasive and, finished with an alumina super-finishing solution. After ultrasonic cleaning, two types of chemical etching were then performed on the cross sections. For observation of the microstructure by optical microscopy or scanning electron microscopy, a Murakami reagent ( $\text{K}_3\text{Fe}(\text{CN})_6/\text{KOH}/\text{H}_2\text{O}$  (1:1:1)) was applied for 3 min while for the observation of carbides, Hasson's reagent ( $\text{C}_2\text{H}_5\text{OH}/\text{HCl}$  (32%)/ $\text{FeCl}_3 \cdot 6\text{H}_2\text{O}$  ( $1300 \text{ g}\cdot\text{L}^{-1}$ ) (3:1:2)) was applied for 2 min. In both cases, the samples were cleaned using distilled water and dried with ethanol.

A standard optical microscope (ZEISS) (Carl Zeiss, Jena, Germany) was used to characterize the microstructure of the SPS sintered samples. The microstructural analysis of the material was carried out using a field emission gun (FEG) scanning electron microscope (SEM JEOL JSM-7600F, Musashino, Akishima, Tokyo, Japan) coupled with a LINK OXFORD energy dispersive X-ray spectrometer (EDXS) (High Wycombe, London, UK) Tensile tests are a suitable method to determine mechanical properties such as the yield strength, the maximum tensile strength and the ductility. Three specimens were extracted from each sintered sample using electrical discharge machining (EDM) as shown in Figure 4. The gauge length and diameter of the gauge section of the samples were 16 and 4 mm, respectively. Uniaxial tensile tests were performed at a constant strain rate of  $10^{-3} \text{ s}^{-1}$  following the ASTM E8/E8M standard test method using a Testwell machine with a 1 MN load cell and a 10 mm long clip gage.

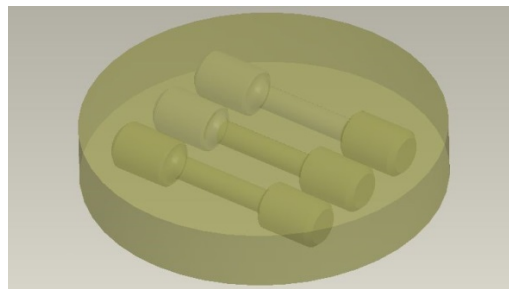


**Figure 4.** Location of the three tensile test pieces machined from within sintered discs (60 mm in diameter and 10 mm in thickness).

### 3. Experimental Results

#### 3.1. Density, Microstructure and Grain Size

Chemical etching on cross-sections of the molybdenum powder consolidated by SPS allows a description of the sintered molybdenum microstructure. Particular attention was paid to following both the evolution of the grain size and the porosity during sintering. An investigation was performed of the growth of the molybdenum grains as a function of the temperature, the holding time and the value of the uniaxial pressure. Figure 5 shows the effect of the sintering temperature (1750, 1900 and 2000  $^{\circ}\text{C}$ ) on the average molybdenum grain size (corresponding to experiments 1, 2, 3 in Table 1, respectively). Thus, a sintered sample at 1750  $^{\circ}\text{C}$  under 90 MPa pressure and without holding time (Figure 5a) has a microstructure with a grain size close to the initial size of the powder particles (i.e., 25  $\mu\text{m}$  determined by laser granulometry). At this temperature, any sign of grain growth is highlighted. By contrast at 1900  $^{\circ}\text{C}$ , grain growth starts but is not homogeneous since two different microstructures are observed: a central part composed of large grains (150  $\mu\text{m}$ , Figure 5c, right hand side) whereas the sample edge is made up of grains having a similar size as initially (i.e., 25  $\mu\text{m}$ , Figure 5c, left hand side). Such an observation is probably the result of a thermal gradient during SPS sintering. The existence of this thermal gradient is due to the absence of a holding time at the sintering temperature which does

not allow thermal homogenization. Effectively, a thermal gradient exists (i.e., as Mo is a conductive material, the center is hotter than the periphery), this latter may be reduced by a modification of SPS tools dimensions and by the addition of graphite felt which limits the thermal losses by radiation [23]. Finally, at 2000 °C, the grain growth occurs over the whole sample (Figure 5b) and the final density is better ( $98.4 \pm 0.2\%$  TMD Theoretical Maximum Density)) in comparison with those obtained at lower temperatures for which the density is not adequate,  $96.5 \pm 0.2\%$  TMD at 1750 °C,  $97.8 \pm 0.2\%$  TMD at 1900 °C without any holding time.

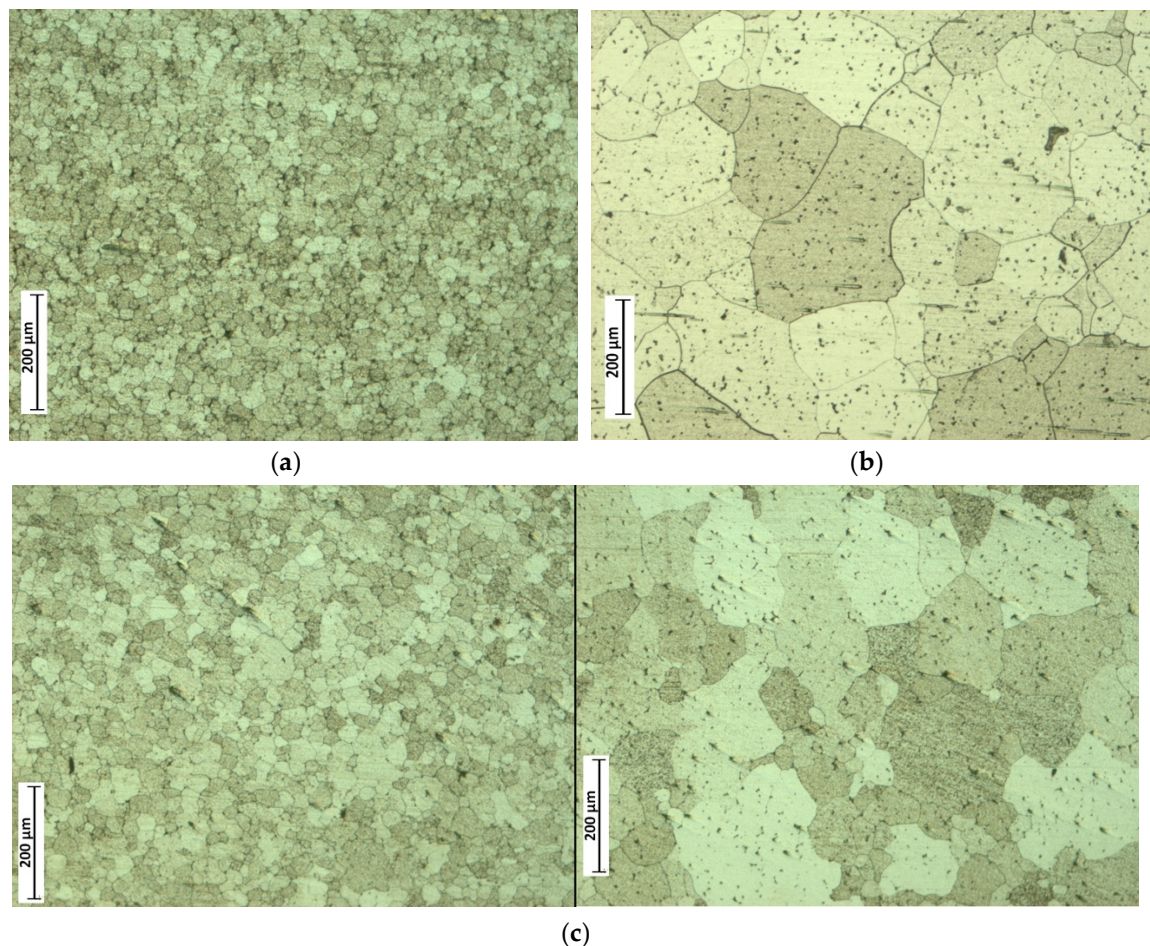


**Figure 5.** Microstructures after chemical etching of molybdenum powder (Mo-45) sintered under 90 MPa pressure without holding time at: (a) 1750, (b) 2000 and (c) 1900 °C (left: edge, right: core).

To evaluate the influence of holding time on molybdenum grain growth, studies were performed at 1900 °C for various holding times (0, 10 and 30 min) under 70 MPa pressure. These tests correspond to experiments 4, 5, 6, in Table 1. As shown in Figure 6b, after 10 min of holding time, the microstructure is different, with an irregular, but generalized grain growth compared to a sintered sample without holding time (Figure 6a). The latter has a fine microstructure on the shell but a beginning of grain growth in the core. After 30 min, the growth is total and regular in the whole sintered sample, as can be seen in Figure 6c. In reality, the grain growth starts after 2 or 3 min at temperature and it is difficult to obtain a microstructural difference between the core and shell. Because of this abrupt change in microstructure, it is possible to qualify this grain growth as exaggerated, in comparison with the phenomena usually observed in metal powders during sintering. The density is also affected by the holding time. While the density of the molybdenum powder after sintering without holding time is around  $98.2 \pm 0.2\%$  TMD, after 10 min this becomes  $99.2 \pm 0.2\%$  TMD and after 30 min, maximum densification is reached, with a density of  $99.9 \pm 0.2\%$  TMD.

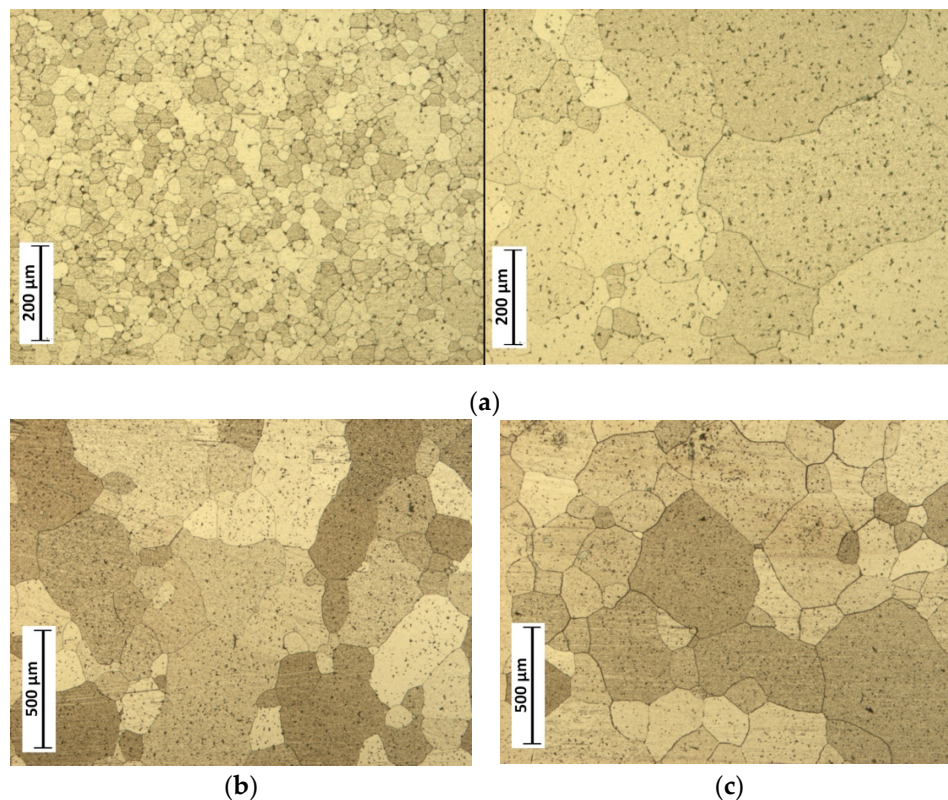


**Figure 6.** Microstructures after chemical etching of molybdenum powder (Mo-45) sintered at 1900 °C under 70 MPa pressure: (a) without holding (left: shell, right: core), (b) 10 min and (c) 30 min.

In addition (Figure 7), the Mo-45 powder, sintered at 1750 °C under 70 MPa pressure and held for 30 min (i.e., corresponding to experiment 7 in Table 1) shows a different microstructure than seen previously at 1900 °C for the same holding time (Figure 6c). The microstructure obtained is close to those obtained at 1900 °C without holding (Figure 5a). In fact, it is necessary to find a good compromise between temperature and holding time to obtain dense molybdenum with homogeneous microstructure while avoiding exaggerated grain growth.

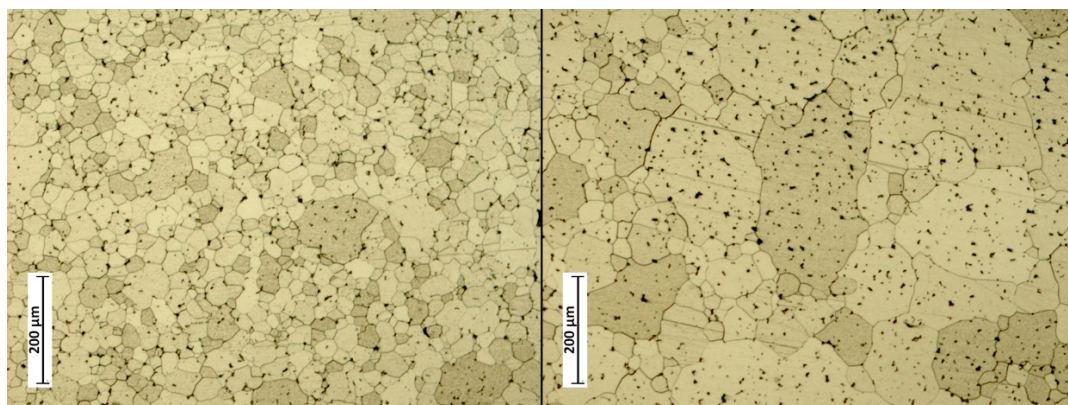


**Figure 7.** Microstructures after chemical etching of molybdenum powder (Mo-45) sintered at 1750 °C under 70 MPa pressure for 30 min (left: shell, right: core). Black dots are due colloidal silica used as reactant.

The influence of the mechanical pressure was also investigated for samples sintered at 1900 °C without holding time. Figures 5c, 6a and 8a show the evolution of molybdenum microstructure for three different pressures, 28, 70 and 90 MPa corresponding to experiments 8, 4 and 2 in Table 1, respectively.

There is no grain growth at 28 MPa even with 30 min of holding time. So at this pressure, the grain growth mechanisms are not activated and the density is limited to  $90.7 \pm 0.2\%$  TMD. But, at and above 70 MPa pressure, the grain growth is similar and seems to be governed by the same driving forces as previously since grain growth and a non-homogeneous microstructure are observed. The density of this sample was close to  $98.2 \pm 0.2\%$  TMD.

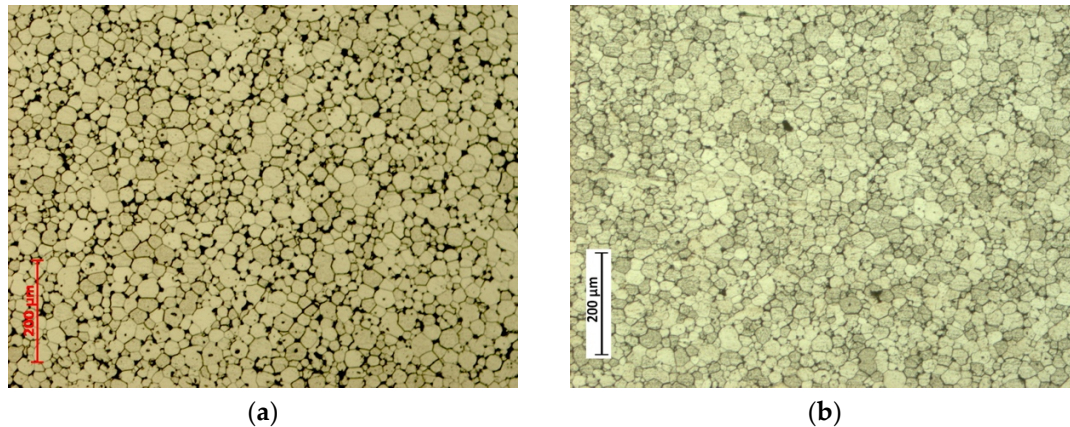


**Figure 8.** Microstructures after chemical etching of molybdenum powder (Mo-45) after sintering at 1900 °C without holding time: (a) under 28MPa and (b) under 70MPa applied at 900 °C.

However, if the pressure is not applied from the beginning of the sintering cycle but at a temperature of 900 °C, for example (i.e., corresponding to experiment 9 in Table 1), the microstructure is affected as shown in Figure 8b. Indeed, grain growth has not occurred and the microstructure is also homogeneous with a density of  $98.1 \pm 0.2\%$  TMD. Several phenomena can explain those microstructural changes, such as the effect of the mechanical pressure which induces plastic deformation (including creep) and, consequently, changes the surface contact between particles leading to a modification of the local temperature.

### 3.2. Diffusion of Carbon

During sintering at 1900 °C under 70 MPa pressure for 30 min (experiment 6 in Table 1), the presence of a carbon layer on the molybdenum surface was demonstrated (Figure 9). This phenomenon has already been highlighted by Mouawad [12]. This layer with a thickness of 100 µm was composed of molybdenum carbides, as experimentally shown by X-Ray Diffraction (XRD). These molybdenum carbides can exist in two stable forms: the  $\alpha$ -Mo<sub>2</sub>C phase and the  $\beta$ -Mo<sub>2</sub>C phase. XRD analysis confirmed that this layer was mainly composed of the hexagonal phase  $\beta$ -Mo<sub>2</sub>C (the  $\alpha$ -Mo<sub>2</sub>C phase is orthorhombic). The thickness of the carbide layers depends on how far the carbon diffuses into the molybdenum, i.e., it depends on the sintering temperature, the holding time and the pressure. However, although this layer of molybdenum carbide leads to a hardness higher than a sample without it, it has proved to be harmful since it is very brittle, which does favor some mechanical properties such as ductility.

The formation of this carbide layer is mainly due to the presence of the graphite foil in contact with the sample and of the SPS chamber environment which is super-saturated with carbon (from the dies, spacers). In order to prevent carbon diffusion, the graphite foil located on the inner part of the die was coated with a boron nitride spray to create a chemical barrier. It also enhances the passage of the electric current inside the sample. However, as it is necessary to preserve the passage of the current within the sample, it is therefore not possible to deposit boron nitride on the surface of each punch. It is difficult to find a pertinent way to protect molybdenum sample surfaces from the formation of this layer, which can be removed easily by sandblasting, but this causes cracking and then the spalling of the molybdenum carbide layer.

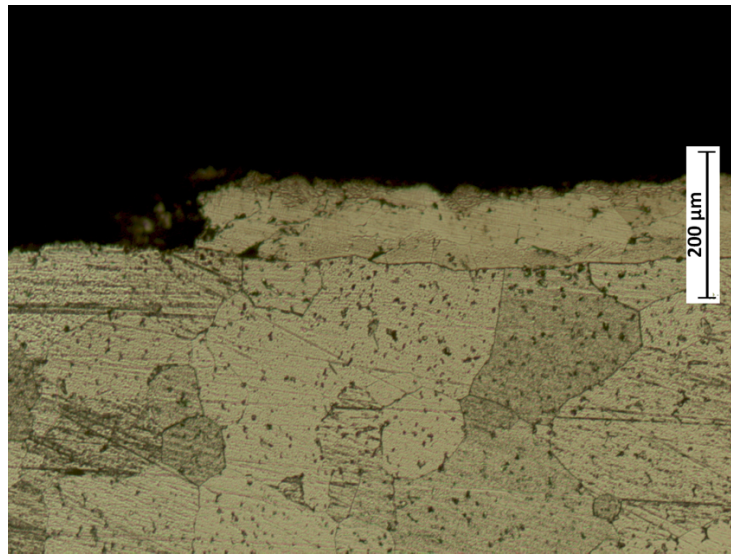


**Figure 9.** Microstructures after chemical etching of molybdenum powder after sintering at 1900 °C under 70 MPa pressure for 30 min showing the carbide layer on the surface.

Unfortunately, the diffusion of carbon is not limited to the first 200 μm of the samples. Chemical etching shows the presence of molybdenum carbides both in the bulk and at the sample periphery. A study of those carbides shows that a relationship exists between the quantity, the location and the form of those carbides and the growth of molybdenum grains during sintering. Indeed, as can be seen in Figure 10a for the case of molybdenum with no grain growth during sintering, internal diffusion of carbon from the sample surface to the bulk and the formation of carbides are not highlighted whereas when grain growth occurs (Figure 10b), carbides are present at grain boundaries.

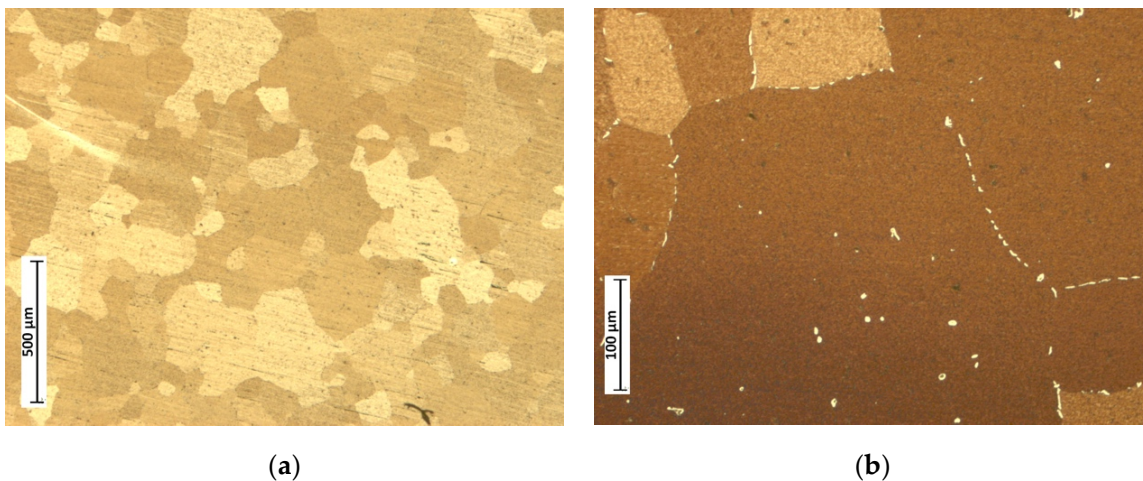


**Figure 10.** Microstructures after chemical etching of molybdenum powder sintered at 1900 °C under 70 MPa pressure: (a) without a holding time and (b) with a 30 min holding time in both cases at the sample centre.

Such carbon diffusion depends not only on the temperature, the holding time and the mechanical charge but also on the sintering environment. To reduce the presence of such carbides, it is essential either to avoid the diffusion of carbon or, if diffusion occurs, the formation of those carbides.

Our observations show that molybdenum carbides form at a high temperature, above 1500 °C, in a carbon saturated environment. At 1900 °C and without a holding time, the diffusion is minimal as is the grain growth but, in that case, the density remains low (<98% TMD ± 0.2%). A first solution is to create a barrier to the diffusion of carbon into samples. Only two materials have a melting point higher

than that of the molybdenum, namely tantalum and tungsten. Two 300 mm thick discs of tantalum were placed on either side of the powder to create a carbon diffusion barrier. This barrier enables the limitation of grain growth by reducing carbon diffusion into the molybdenum and, consequently, the formation of molybdenum carbides. This barrier is efficient because for sintering at 1900 °C under 70 MPa pressure for 30 min, there is no diffusion, no formation of carbide and no molybdenum grain growth (Figure 11).

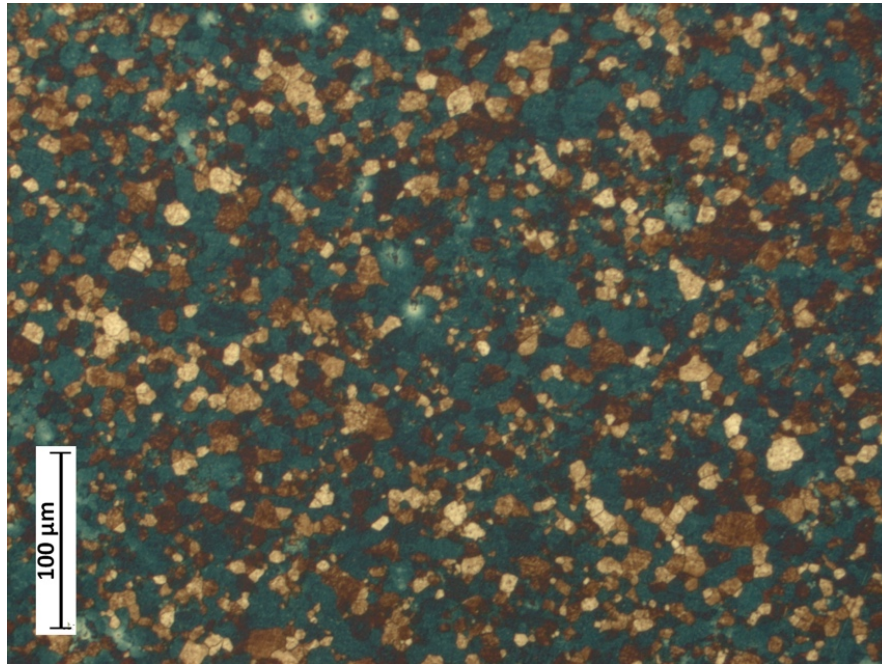


**Figure 11.** Microstructure after chemical etching of molybdenum sintered at 1900 °C under 70 MPa pressure, for a holding time of 30 min with a 3 mm tantalum barrier.

This solution shows clearly that it is essential to avoid long distance carbon diffusion. Consequently, the presence of carbon or carbides changes the grain growth mechanisms. However, this solution is expensive and non-reusable because tantalum carbides are formed, and is difficult to adapt to the sintering of complex shapes.

As the relationship between carbides and grain growth was unclear, new experiments were performed using a commercial molybdenum powder containing a high concentration of carbon. This powder is also produced by the TEKNA company (Mâcon, France) (the commercial name is Mo-45 HC) and the carbon concentration is controlled during the ICP process). This powder, which has a similar particle size as the previously studied powder (Mo-45), is composed of two phases: Mo and Mo<sub>2</sub>C. Sintering of the Mo-45HC powder at 1900 °C under 70MPa pressure for 30 min and without a tantalum diffusion barrier produces a fine microstructure (Figure 12), with a grain size close to the initial particle size of the powder grain. The molybdenum carbides do not seem to be responsible for the exaggerated grain growth but the “free” carbon plays a role in this phenomenon.



**Figure 12.** Microstructures after chemical etching of molybdenum powder with a high carbon content after sintering at 1900 °C under 70 MPa pressure for 30 min of holding.

### 3.3. Presence of Oxygen

XPS analysis performed on the molybdenum powder showed the presence of a thin layer (~4–5 nm) of molybdenum oxides at the grain surface. However, an exact measurement of the oxygen content in the bulk material after sintering remains difficult to obtain. In addition, the effect of this layer on the evolution of microstructure during sintering is uncertain. That is why, to amplify the effect of oxygen, a molybdenum powder was used with a particle size ranging from 3–7  $\mu\text{m}$  (i.e., high surface area) and made without control of the oxygen concentration (produced by Alfa Aesar and named Mo-1). This powder has a smaller particle size than the previous ones, so the sintering temperature is lower. After a sintering cycle at 1750 °C under 70 MPa pressure (hold time 10 min) and using a tantalum diffusion barrier (disc of 3 mm thick), the microstructure did not show any grain growth or any molybdenum carbides. However, observation of the intergranular brittle fracture surfaces of this part (Figure 13a) shows the presence of a high concentration of spheres, composed of molybdenum oxides, i.e.,  $\text{MoO}_2$  and  $\text{MoO}_3$ .

In order to reduce the amount of molybdenum oxides, it was decided to add a reduction stage composed of a 650 °C temperature plateau lasting 30 min in vacuum before the sintering stage. After fracture of the sample, the surfaces (Figure 13b) also are characteristic of brittle fracture but there are no oxides at the grain surface. The reduction stage in vacuum is effective since an exaggerated grain growth, with grain sizes ten times larger than the initial grain size is observed. The spherical molybdenum oxides seem to block the grain boundaries, preventing exaggerated grain growth. The elimination of these oxides releases the grain boundaries and allows grain growth to occur.

Then, in order to limit the grain growth and to avoid the use of a tantalum barrier (i.e., limit the carbon diffusion), a sintering cycle composed of an oxide reduction stage at 650 °C and sintering at a temperature lower to that relative to carbide formation (i.e., 1450 °C) was carried out. These processing conditions produce a molybdenum disc without oxides and without grain growth (Figure 13c). Even if the oxide reduction stage is efficient, the effect of temperature remains non-negligible on the grain growth and also on the density ( $95.5 \pm 0.2\%$  TMD).

At high temperature, carbon strongly reduces molybdenum oxides. The diffusion of “free” carbon from the matrix to the center of the molybdenum grains induces the reduction of the molybdenum trioxides and dioxides if these have not been eliminated during the reduction stage performed in vacuum. These reductions release the grain boundaries. Several reactions occur, as described by Hegedus and Neugebauer [24], leading to the formation of some gaseous phases ( $\text{CO}$ ,  $\text{CO}_2$ ), which can

be observed on the fracture surfaces of the powders sintered at high temperature with a finite holding time but without a reduction stage (Figure 14).

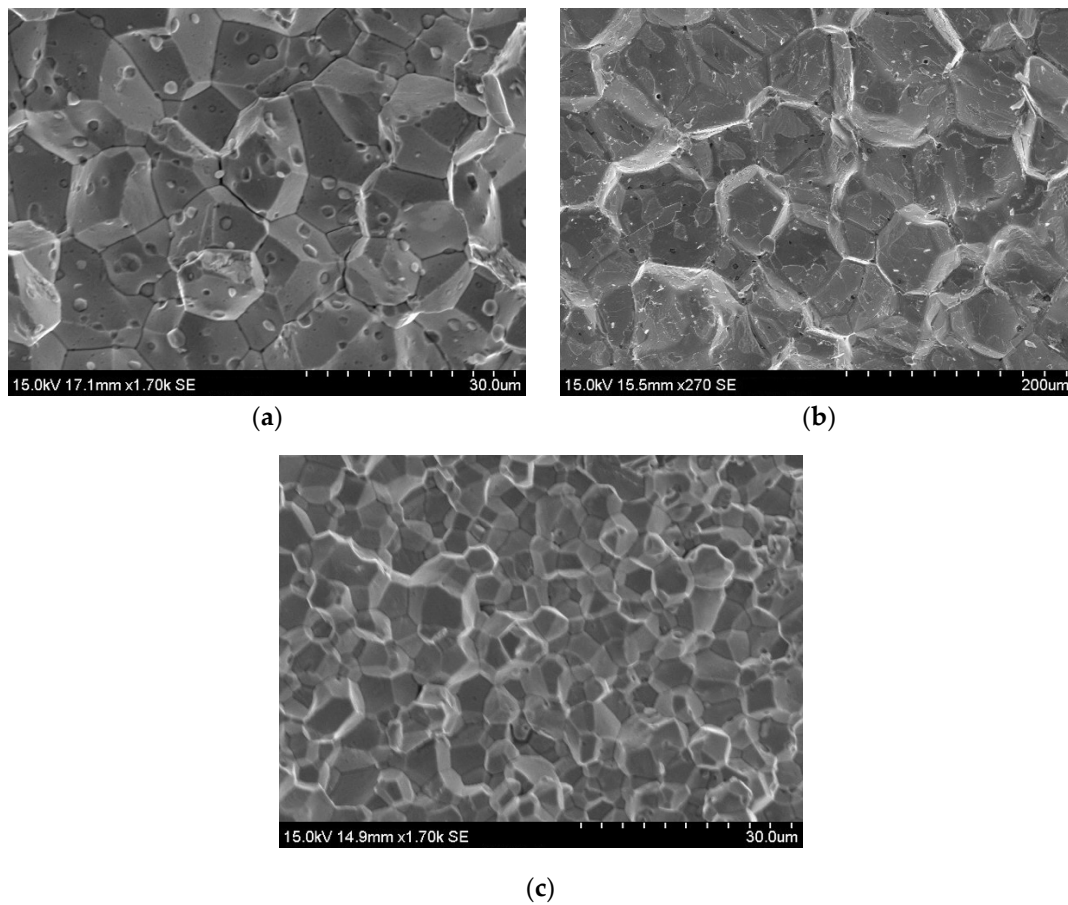


**Figure 13.** Fracture surfaces of high-oxidized sintered molybdenum: (a) at 1750 °C without reduction stage, (b) at 1750 °C and with an oxide reduction plateau at 650 °C and (c) at 1450 °C with an oxide reduction plateau at 650 °C.

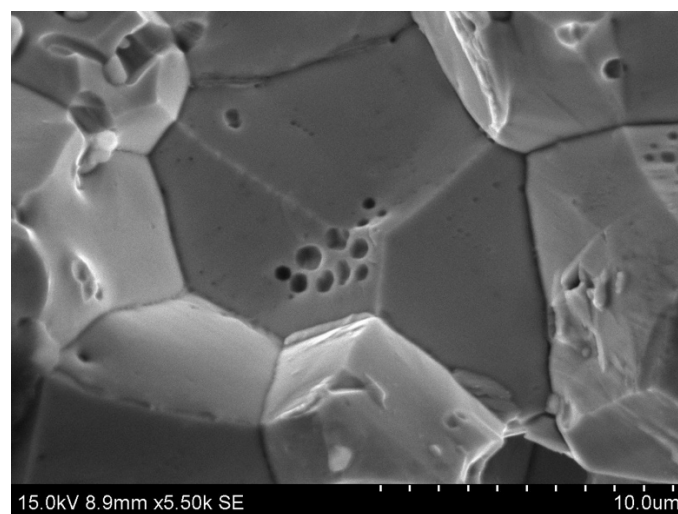


**Figure 14.** Fracture surfaces of sintered molybdenum powder at 1450 °C under 70 MPa during 30 min without reduction stage at 650 °C, showing the effect of gaseous species.

After the reduction reaction between carbon and the molybdenum oxides, the excess carbon continues to diffuse into the sample and reacts with the molybdenum to form some carbides. These carbides are responsible for the high fragility of the material. The ideal sintered molybdenum is a dense solid without oxides and carbides. For the first species, an oxide reduction stage can be implemented in the sintering cycle, but at high temperature, which is a necessary condition to obtain high density, exaggerated grain growth is observed. This heterogeneous microstructure penalizes the mechanical properties of the final product. As for the carbides, the diffusion of carbon can be limited by the use of a tantalum barrier. However, this solution is not economically or technically feasible for the production of large and complex parts. For control of both of these impurities, sintering at a temperature lower than 1500 °C seems to be a good solution but these latter are not dense ( $\sim 90\%$  TMD  $\pm 0.2\%$ ). Indeed, below this temperature, carbides do not form and if a reduction stage is implemented, the microstructure remains fine-grained without grain growth. However, it is still possible that some carbon diffusion occurs. However, the diffusion is slow, so even if it occurs, it remains limited.

In the case of the dense molybdenum produced from commercial powder made by Tekna, this sintering temperature is an interesting way of solving the carbide formation; however, its density is not sufficient (density close to  $90\%$  TMD  $\pm 0.2\%$ ), meaning another solution has to be found. Several possibilities can be envisaged, such as a powder with smaller grains or a mechanically activated powder, but in both cases, the purity of the powder remains essential.

#### 3.4. Mechanical Activation

As shown previously, a sintering temperature below 1500 °C is needed to limit grain growth and carbide formation. However, a lower temperature means a lower density and usually poor mechanical properties. Mechanical activation is a means of lowering the sintering temperature by reducing the sintering activation energy.

The ball milling stage (i.e., Fritsch pulverisette 4 planetary ball mill) was carried out using hardened steel balls which are introduced inside vials made of hardened steel. Planetary ball milling is characterized by two rotations expressed in rotations per minute (rpm): (i) rotation  $\Omega$  of the plate to which the vials are fixed to obtain centrifugal acceleration, and (ii) rotation  $\omega$  of the vials in the opposite direction. Depending on the selected rotation speeds, it is possible either to promote collisions or friction (energy and frequency of shocks) [25,26]. Moreover, the vials are filled in a glove box under an argon atmosphere in order to avoid oxidation. The molybdenum powders were ground according to the condition  $\Omega/\omega/h = 250 \text{ rpm}/-250 \text{ rpm}/4 \text{ h}$  (i.e., friction mode). The size distribution of the commercial powder ranges from 10–30 to 10–75  $\mu\text{m}$  after milling confirming the formation of nanostructured agglomerates as we have seen in the case of copper [25]. On the other hand, the agglomerates are smaller because of the more fragile character of molybdenum (Figure 15).

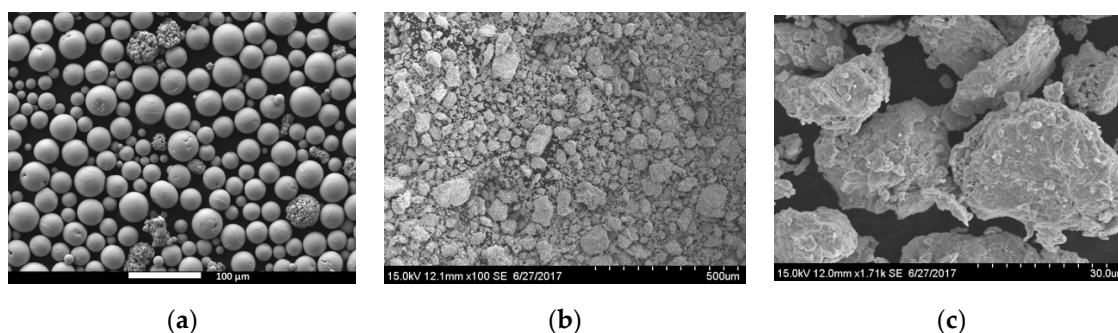


**Figure 15.** SEM microstructural analysis of commercial Mo-45 powders (a) and mechanically activated molybdenum powder agglomerates (b,c); (b) overview of the agglomerates showing that they can reach a size greater than 50  $\mu\text{m}$ , and (c) observation of mechanically activated agglomerates.

X-ray diffraction patterns of powders that were mechanically activated by milling show a significant broadening of the XRD peaks corresponding to a decrease in the size of the crystallites and an increase in structural defects when high energy milling is applied. The influence of mechanical milling on the sintering behavior is confirmed by the curves in Figure 16 which compares the shrinkage curve of unmilled commercial powder shown as a solid green line (the solid red curve corresponds to the densification speed) and that for mechanically activated powder shown as a dotted green line (the dotted red curve corresponds to the densification speed). In fact, this figure shows that sintering begins at a lower temperature, that it is more active (higher slope) and that it finishes before 1500 °C, a temperature not to be exceeded to avoid the formation of molybdenum carbides and oxides. In addition, using the master curves method Lorand [27] has shown that high-energy mechanical grinding induces a decrease in the activation energy of sintering ( $Q = 195$  kJ/mol instead of  $\sim 330$  kJ/mol) due to the presence of structural defects.

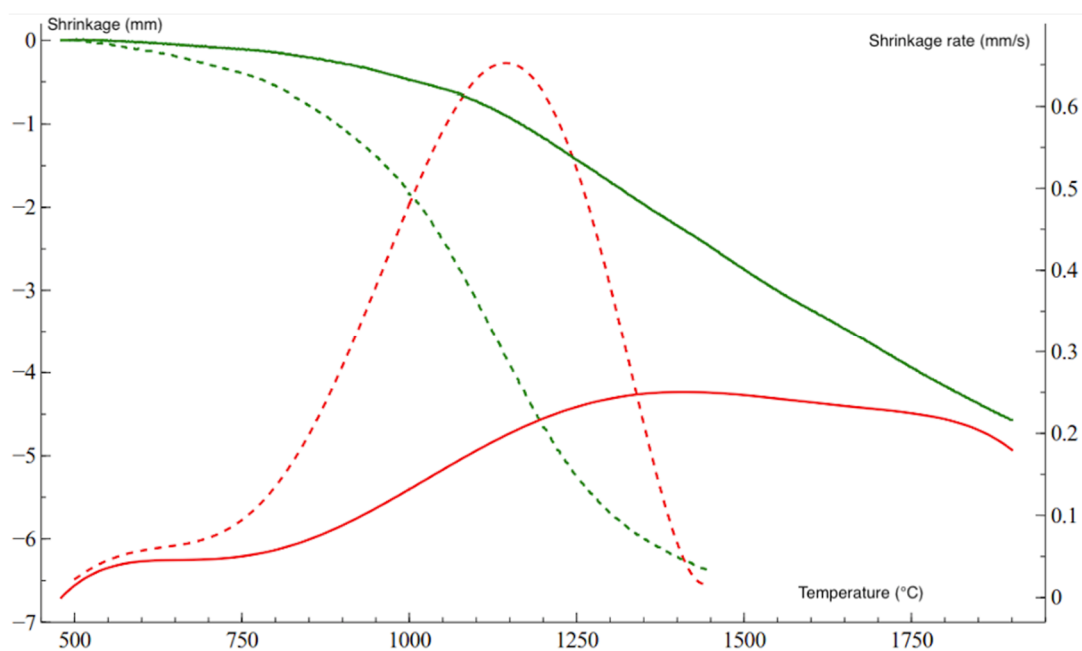


**Figure 16.** Shrinkage curves and densification speed for an unmilled Mo-45 powder (solid line, green shrinkage, red speed) and mechanically activated Mo powder (dotted line green shrinkage, speed in red). This figure clearly shows the advantage of milling to modify the sintering conditions of molybdenum powder.

SPS sintering of a mechanically activated molybdenum powder under the conditions 1450 °C, 70 MPa pressure for 30 min led to the formation of a dense molybdenum ( $98.7 \pm 0.2\%$  TMD) having a fine microstructure with no carbides or oxides. The formation of carbides is avoided if the sintering temperature is smaller than 1500 °C. However, the presence of free carbon may be interesting because this latter in low concentration enables the increasing of the Mo ductility [17,18].

Tensile tests have been carried out on samples sintered from unmilled and from mechanically activated powders (Figure 17a). The tensile test results highlight the improvement of ductility after ball milling, as a ductility of 13% was reached. We are in presence of a particular ductile failure process, encountered with BCC systems, with a cleavage fracture triggered after local plastic deformation. This cleavage process consists in plastic deformation of the crystal grains, the “ductile” aspect, followed by a transgranular failure of parallel dense atomic planes revealing facet with river appearances, the “cleavage” aspect of dense planes without dimples. This particular ductile failure process has been observed with tungsten particles, BCC as molybdenum, as reported by Lankford et al. [28]. In this work the ductile failure process has been called “transgranular shear cleavage”.

However, some pores remain after sintering (Figure 17b). These results show the efficiency of the milling process since it reduces the sintering temperature and so avoids carbide formation. This is confirmed by the ductility of the sintered molybdenum. The large difference in the elastic limit of the unmilled powder (near 500 MPa) and milled powder (about 300 MPa) compacts comes from that the grain growth during sintering of the milled powder is greater than with as received powder. Precisely, the unmilled microstructure reveals a grain size of about 10  $\mu\text{m}$ , while the grain size of the milled microstructure has been estimated at 7  $\mu\text{m}$ . Such grain size data apply to the Hall Petch relation, along with the yield stress data of Figure 17a.

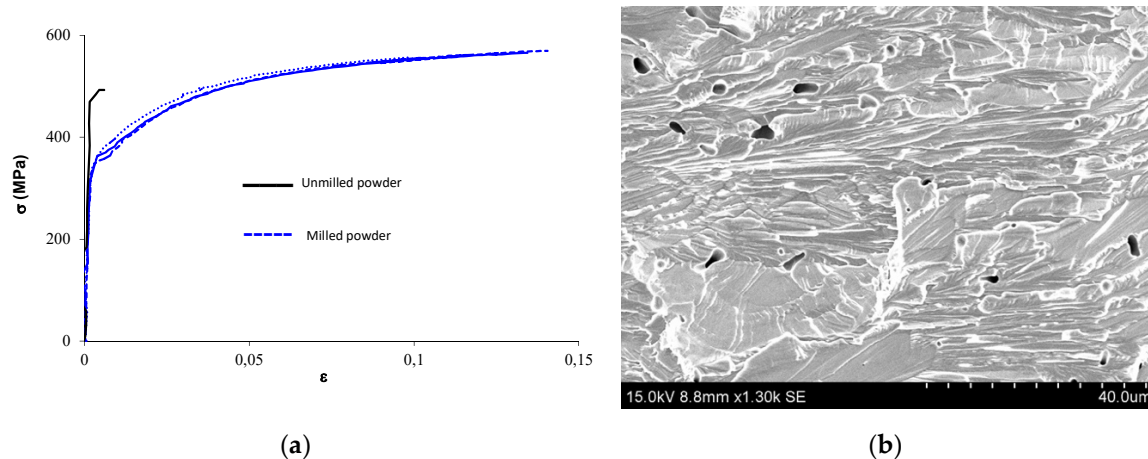


**Figure 17.** (a) True tensile stress strain curves of molybdenum samples sintered from unmilled and milled powder (b) SEM image of fracture surface of a sintered milled powder.

#### 4. Conclusions

When oxygen is present as an oxide in the bulk material, the molybdenum grain boundaries are locked, thus preventing grain growth of the molybdenum grains, an undesirable effect during sintering. In addition, this pollution is prejudicial for the purity of the final product as well as for its mechanical properties. Therefore, it is necessary to remove any trace of oxygen during sintering by application of an oxide reduction stage. This can be done by the addition of carbon via the diffusion from the graphite present in the SPS tools. However, the formation of a carbide phase is also prejudicial to molybdenum for the same reasons as the oxide. It is therefore necessary to go through an oxide reduction stage and to add protection against carbon diffusion in order to obtain dense molybdenum with a pure chemical composition. It has been shown that the solution of introducing a barrier against diffusion of carbon is not viable for SPS sintering especially in the case of complex shapes. Moreover, by eliminating oxygen, densification will inevitably lead to exaggerated grain growth. The coarser microstructure of molybdenum so formed will then affect the mechanical properties of the final part.

Sintering temperature conditions with oxide reduction and no carbon diffusion are therefore required. This can be hypothetically performed if during sintering an oxide reduction stage at 650  $^{\circ}\text{C}$  is added, and if sintering is carried out below the carbide formation temperature, i.e., at a temperature lower than 1500  $^{\circ}\text{C}$ . However, for a temperature below 1500  $^{\circ}\text{C}$ , the final product is not dense enough. The solution adopted to meet this challenge was to implement high energy mechanical milling of the molybdenum powder. SPS sintering of a mechanically activated molybdenum powder according to the conditions 1450  $^{\circ}\text{C}/30\text{ min}/70\text{ MPa}$  has been performed. This mechanical activation of molybdenum powders led to the formation of a dense product (98.7% TMD) having a fine microstructure without either carbides or oxides. A ductility close to 13% could be reached via the observation of transgranular rupture still containing a few pores resulting from mechanical activation. Our results are very encouraging, because the tensile properties  $R_m = 550\text{ MPa}$  and  $A\% = 13\%$  of the raw SPS products are comparable to those obtained by Plansee for a sintered and annealed molybdenum ( $R_m = 560\text{ MPa}$  and

14%). On the other hand, they are much lower than those obtained in sintered, forged and annealed products for which a ductility of 40% has been obtained [1]. Consequently, it will be essential to perform further SPS sintering investigations so as to improve the ductility, while keeping in mind that the SPS approach provides a unique advantage compared to other processes with the ability to elaborate near shape parts.

**Author Contributions:** Methodology, M.M. and F.B. (Florian Bussiere); validation, S.L. and F.D.; formal analysis, F.B. (Frédéric Bernard) and H.C.; writing—original draft preparation, M.M. and S.L.; writing—review and editing, F.D., F.B. (Frédéric Bernard) and H.C.; supervision, F.B. (Frédéric Bernard) and H.C. All authors have read and agreed to the published version of the manuscript.

**Funding:** The authors thank the Regional Council of Bourgogne Franche-Comté for funding the Ph.D. grant of Sylvain Lorand Ph-D, and the French MOD for funding the Ph.D. grant of Mathias Moser.

**Acknowledgments:** Specific thanks to Stephen Walley from Cambridge University for his valuable comments.

**Conflicts of Interest:** The authors declare no conflict of interest.

## References

- Lichtenberger, A. Ductile behavior of some materials in the shaped charge jet. In *Metallurgical and Materials Applications of Shock-Wave and High-Strain-Rate Phenomena*; Murr, L.E., Staudhammer, K.P., Meyers, M.A., Eds.; Marcel Dekker: New York, NY, USA, 1995; pp. 463–470.
- Kim, Y. Consolidation behavior and hardness of P/M molybdenum. *Powder Technol.* **2008**, *186*, 213–217. [[CrossRef](#)]
- Park, H.-K.; Ryu, J.-H.; Youn, H.-J.; Yang, J.-M.; Oh, I.-H. Fabrication and property evaluation of Mo compacts for sputtering target application by spark plasma sintering process. *Mater. Trans.* **2012**, *53*, 1056–1061. [[CrossRef](#)]
- Sakamoto, T. Sintering behavior of Mo powder compact applied SPS spark plasma sintering method. *J. Jpn. Soc. Powder Metall.* **1997**, *44*, 845–850. [[CrossRef](#)]
- Garg, P.; Park, S.-J.; German, R.M. Effect of die compaction pressure on densification behavior of molybdenum powders. *Int. J. Refract. Met. Hard Mater.* **2007**, *25*, 16–24. [[CrossRef](#)]
- Kim, G.-S.; Kim, H.G.; Kim, D.-G.; Oh, S.-T.; Suk, M.-J.; Kim, Y.D. Densification behavior of Mo nanopowders prepared by mechanochemical processing. *J. Alloy. Compd.* **2009**, *469*, 401–405. [[CrossRef](#)]
- Srivatsan, T.S.; Ravi, B.G.; Petraroli, M.; Sudarshan, T.S. The microhardness and microstructural characteristics of bulk molybdenum samples obtained by consolidating nanopowders by plasma pressure compaction. *Int. J. Refract. Met. Hard Mater.* **2002**, *20*, 181–186. [[CrossRef](#)]
- Kim, Y.; Lee, S.; Noh, J.-W.; Lee, S.H.; Jeong, I.-D.; Park, S.-J. Rheological and sintering behaviors of nanostructured molybdenum powder. *Int. J. Refract. Met. Hard Mater.* **2013**, *41*, 442–448. [[CrossRef](#)]
- Murr, L.E.; Tuominen, S.M.; Hare, A.W.; Wang, S.-H. Structure and hardness of explosively consolidated molybdenum. *Mater. Sci. Eng. A* **1983**, *57*, 107–111. [[CrossRef](#)]
- Shankar, S.; Murr, L.E. Heat treatment of explosively consolidated molybdenum: TEM studies. *J. Mater. Sci. Lett.* **1984**, *3*, 15–17. [[CrossRef](#)]
- Chhillar, P.; Agrawal, D.; Adair, J.H. Sintering of molybdenum metal powder using microwave energy. *Powder Metall.* **2008**, *51*, 182–187. [[CrossRef](#)]
- Mouawad, B.; Soueidan, M.; Fabregue, D.; Buttay, C.; Bley, V.; Allard, B.; Morel, H. Full densification of Molybdenum powders using spark plasma sintering. *Metall. Mater. Trans. A* **2012**, *43*, 1–8. [[CrossRef](#)]
- Ohser-Wiedemann, R.; Martin, U.; Seifert, H.J.; Müller, A. Densification behaviour of pure molybdenum powder by spark plasma sintering. *Int. J. Refract. Met. Hard Mater.* **2010**, *28*, 550–557. [[CrossRef](#)]
- Huang, H.S.; Hwang, K.S. Deoxidation of molybdenum during vacuum sintering. *Metall. Mater. Trans. A* **2002**, *33*, 657–664. [[CrossRef](#)]
- Krajcnikov, A.V.; Drachinskiy, A.S.; Slyunyaev, V.N. Grain boundary segregation in recrystallized molybdenum alloys and its effect on brittle intergranular fracture. *Int. J. Refract. Met. Hard Mater.* **1992**, *11*, 175–180. [[CrossRef](#)]
- Kumar, A.; Eyre, B.L. Grain boundary segregation and intergranular fracture in molybdenum. *Proc. R. Soc. Lond. A Math. Phys. Eng. Sci.* **1980**, *370*, 431–458.

17. Hiraoka, Y. Significant effect of carbon content in the low-temperature fracture behavior of molybdenum. *Mater. Trans. JIM* **1990**, *31*, 861–864. [[CrossRef](#)]
18. Kadokura, T.; Hiraoka, Y.; Yamamoto, Y.; Okamoto, K. Change of mechanical property and fracture mode of molybdenum by carbon addition. *Mater. Trans.* **2010**, *51*, 1296–1301. [[CrossRef](#)]
19. Hofmann, H.; Grosskopf, M.; Hofmann-Antenbrink, M.; Petzow, G. Sintering behaviour and mechanical properties of activated sintered molybdenum. *Powder Metall.* **1986**, *29*, 201–206. [[CrossRef](#)]
20. Hwang, K.S.; Huang, H.S. Identification of the segregation layer and its effects on the activated sintering and ductility of Ni-doped molybdenum. *Acta Mater.* **2003**, *51*, 3915–3926. [[CrossRef](#)]
21. Zovas, P.E.; German, R.M. Retarded grain boundary mobility in activated sintered molybdenum. *Mater. Trans. A* **1984**, *15*, 1103–1110. [[CrossRef](#)]
22. Lee, B.-K.; Oh, J.-M.; Shon, I.-J.; Kim, H.-S.; Lim, J.-W. Influence of oxygen concentration on mechanical properties of molybdenum powder during sintering. *J. Nanosci. Nanotechnol.* **2014**, *14*, 9029–9032. [[CrossRef](#)] [[PubMed](#)]
23. Naimi, F.; Ariane, M.; Barthelemy, F.; Cury, R.; Mahot, P.; Couque, H.; Bernard, F. The hybrid-SPS, an effective tool to produce large-sized parts. In *Spark Plasma Sintering: Current Status, New Developments and Challenge Dedicated to Prof. Z.A. Munir*; Cao, G., Orru, R., Estournés, C., Garay, J., Eds.; Elsevier: Amsterdam, The Netherlands, 2019; pp. 301–312.
24. Hegedüs, A.J.; Neugebauer, J. Zum mechanismus der reaktion von molybdäntrioxyd mit kohlenstoff. *Z. Anorg. Allg. Chem.* **1960**, *305*, 216–226. [[CrossRef](#)]
25. Gaffet, E.; Bernard, F. Mechanically activated powder metallurgy processing: A versatile way towards nanomaterials synthesis. *Ann. Chim. Sci. Mat.* **2002**, *27*, 45–59.
26. Boytsov, O.; Gaffet, E.; Bernard, F.; Ustinov, A. Correlation between milling parameters and microstructure characteristics of nanocrystalline copper powder prepared via a high energy planetary ball mill. *J. Alloy. Compd.* **2007**, *432*, 103–110. [[CrossRef](#)]
27. Lorand, S. Maitrise De La Microstructure Du Molybdène: De La Poudre Préparée Par ICP Au Massif Fritté Par SPS. Ph.D Thesis, Université de Bourgogne, Dijon, France, November 2017.
28. Lankford, J.; Couque, H.; Bose, A.; German, R. Dynamic deformation and failure of tungsten heavy alloys. In *Tungsten and Tungsten Alloys—Recent Advances TMS Conference*; Crownson, A., Chen, E.S., Eds.; The Minerals, Metals & Materials Society: Warrendale, PA, USA, 1991; pp. 151–159.



© 2020 by the authors. Licensee MDPI, Basel, Switzerland. This article is an open access article distributed under the terms and conditions of the Creative Commons Attribution (CC BY) license (<http://creativecommons.org/licenses/by/4.0/>).